IS-4750
UC-90

Alloy Evaluation for Fossil Fuel Process Plants (Liquefaction)

Quarterly Report for

Period

1 April, 1980 through 30 June, 1980

C. M. Woods and T. E. Scott

AMES LABORATORY

Iowa State University

Ames, Iowa 50011

July 15, 1980

PREPARED FOR THE UNITED STATES DEPARTMENT OF ENERGY
UNDER CONTRACT NO. W-7405-Eng-82, WPAS NO. AA-15-10-10

FOREWORD

This report covers work performed during the period 1 April, 1980 through 30 June, 1980. The work was funded by the Office of Advanced Research and Technology under the Assistant Secretary for Fossil Energy and was monitored by R. A. Bradley, Manager of Fossil Energy Materials Projects at Oak Ridge National Laboratory. The report was prepared by Charles M. Woods and T. E. Scott of the Mechanical Properties Section in the Metallurgy and Ceramics Division at the DOE-Ames Laboratory, Ames, Iowa.

The work was performed under the direction of Dr. Scott as principal investigator assisted by: C. M. Woods, S. Shei, C. V. Owen and L. K. Reed.

ABSTRACT

The average thermal expansion coefficient for Carpenter 883 (H-13, the bolt material for bolt loaded compact tension specimens) was determined for the temperature range 72°F to 800°F. The thermal stability, as a function of time, was determined at 800°F. The average thermal expansion coefficients for both A387-74A-Gr.22-Cl.2 steel and 316 stainless steel were determined for the 72°F to 1000°F temperature range. Thermal stability of A387 at 1000°F was monitored for a period of 250 hours. Ring-sample relaxation tests were run in argon at 1000°F for 250 hours. Sample stress versus deflection calibration curves were determined for 316 stainless steel loading rings at 76, 200, 400, 600, 820 and 1000°F. Ring compliance constants (K_r) were determined and plotted versus temperature. Compliance curves for bolt loaded compact tension specimens (BLCTS) were determined at

room temperature and 800°F for three different crack lengths (a). Two BLCTS were loaded and exposed to the coal slurry environment. Corrosion specimens were loaded along with the BLCTS. Both tests were aborted after ∿200 hours due to a rupture disk failure. Smooth-bar and notched-bar tensile specimens of A387-74A-Gr.22-Cl.2 steel were exposed to 4000 psig H_2 gas at 1000°F for 168, 250 and 500 hours. Samples were exposed in the unstressed, stressed, and prestrained conditions. Tensile tests were made in air at room temperature at the end of each exposure. Metallographic examinations were made of fracture surfaces as well as other exposed specimens not subjected to the tensile testing. The exposed material exhibited a marked reduction in notch ductility as well as a small reduction in notch tensile strength. The smooth-bar samples showed no significant changes in mechanical properties even after 500 hours of exposure. SEM examinations revealed the presence of small bubbles that formed mostly on or near grain boundaries and in the vicinity of second phase particles. Specimens cleaved at liquid nitrogen temperature exhibited bubbles on the fracture surface.

Fatigue crack growth rates (da/dN) were determined for a wide variation of stress intensity range values (ΔK). Testing was done in hydrogen gas at ambient temperature and various pressures. Near-threshold to rapid crack growth stages were examined.

OBJECTIVE AND SCOPE

The objective of this program is to evaluate the mechanical properties of liquefaction process plant "dissolver" vessel materials in a "dissolver" vessel environment including coal slurry and pressurized hydrogen gas at temperatures up to 800°F. Originally, the intent was to test at 900°F but we soon learned that above 850°F (455°C) gasification is ignited giving coke and methane. Consequently, all runs originally indicated as 900°F will be run at 800°F to assure there are no excursions above the critical gasification ignition temperature.

Specifically, the degradation of notched-bar and smooth-bar tensile samples of 2 1/4 Cr-1 Mo will be monitored as a function of exposure time and stress in the "dissolver" vessel environment. Compact tension specimens will be used to monitor the degradation of fracture properties in the "dissolver" vessel environment.

Notched-bar tensile specimens will be used to evaluate the behavior of 2 1/4 Cr-1 Mo steel in pure hydrogen gas at various temperatures and pressures. The objective is to determine the Nelson curve.

PROGRESS SUMMARY

I. Thermal Expansion, Thermal Stability, and Compliance Tests

A. Procedure and Results:

Loading bolts for the 2 1/4 Cr-1 Mo bolt-loaded compact tension specimens (Fig. 1) were machined from a 1 1/4" rod of Carpenter 883 tool steel. The bolts, along with bolt rests (Fig. 1) and a thermal expansion specimen of the same material, were packed in gray iron chips and placed in a muffle

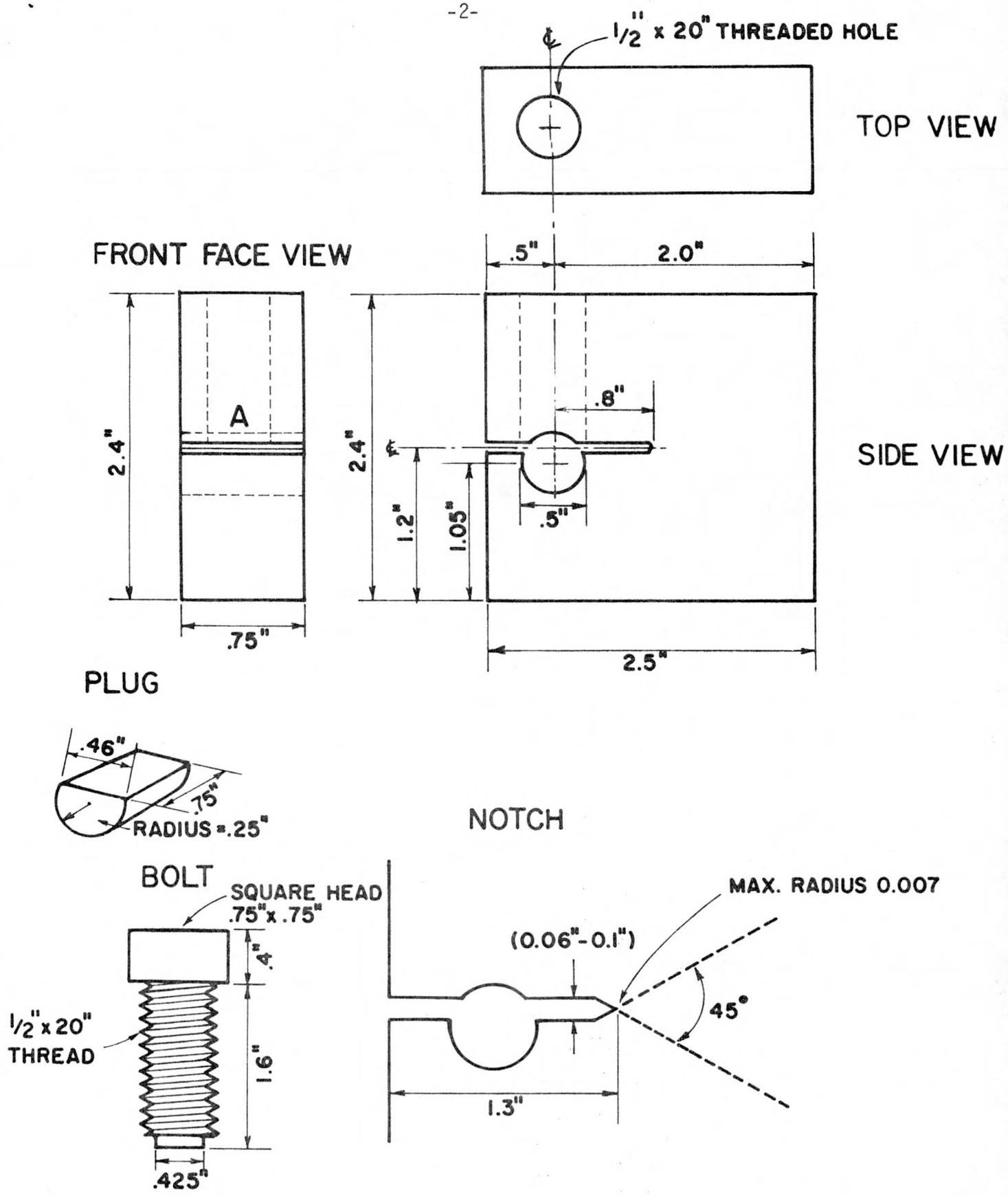

Fig. 1: 2 1/4 Cr-1 Mo Bolt-Loaded Compact Tension Specimen. All dimensions are in inches.

furnace. The iron chips, bolts etc. were heated to 1875°F and held for 25 minutes. The parts were withdrawn from the furnace, removed from the gray iron chips and air cooled in still air to room temperature. The parts were then triple drawn (tempered) at 1025°F for two hours per draw with air cooling to room temperature between draws. The thermal expansion specimen was placed in a quartz thermal expansion rig and the average thermal expansion coefficient was determined for the temperature range 72°F to 800°F. The thermal expansion rig incorporates a capacitance gage having a resolution of 4×10^{-7} inches. The result is listed in Table 1. The specimen was then isothermally held at 800°F in argon and the specimen length monitored for 168 hours. The thermal stability is shown in Figure 2.

Average thermal expansion coefficients for both A387-74A-Gr.22-Cl.2 steel and 316 stainless steel were determined, using the above mentioned rig, for the 72 to 1000°F temperature range. These values are listed in Table 1. The A387 was placed in the test rig and isothermally held in argon at 1000°F for 250 hours. The sample showed good stability as demonstrated in Figure 3.

Ring-sample composite (Fig. 4) relaxation was monitored in argon at 1000°F for 250 hours. The ring was loaded in compression at room temperature in a compression cage on a TT-C Instron tensile test machine. The load was transferred to a notched-bar tensile sample (Fig. 5) spanning the diameter of the pre-compressed ring by screwing the sample into the threaded section of the ring at one end and tightening a nut at the other end. The diameter of the ring was measured before and after loading and adjustments were made to achieve a predetermined value of ring deflection. The ring-sample composite was placed in a specially designed quartz thermal

TABLE #1

THERMAL EXPANSION DATA

Temperature Range (°F)	Material	Thermal Expansion Coefficient (μ in/in/°F)
72-500	A387	7.03±.04
72-800	A387	7.43±.02
72-900	A387	7.48±.02
72-1000	A387	7.53±.02
72-500	316 SS	9.54±.05
72-800	316 SS	9.87±.02
72-900	316 SS	9.93±.01
72-1000	316 SS	10.16±.01
72-800	883 (H-13)	7.07±.02

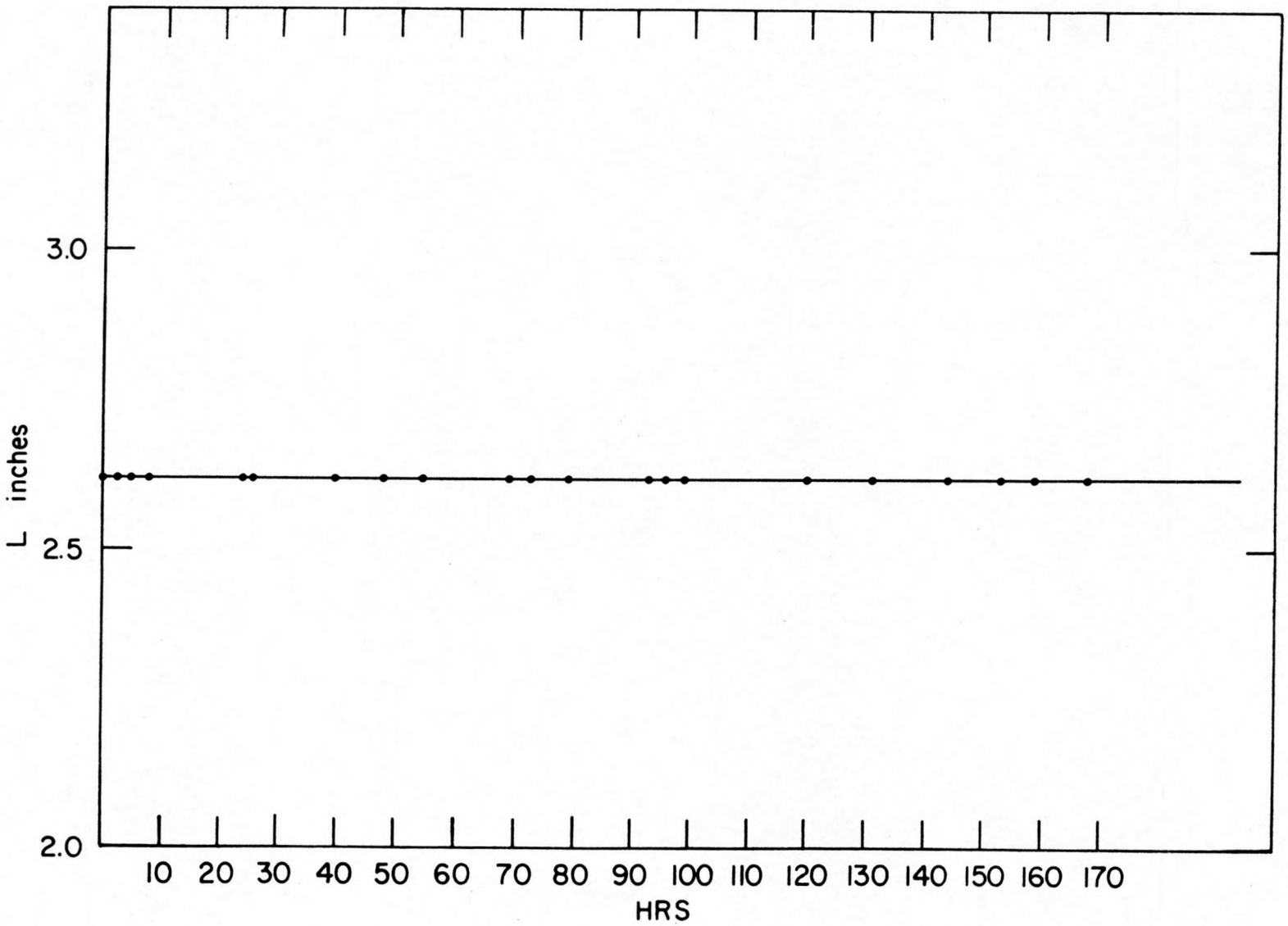

Fig. 2: Plot of thermal stability of Carpenter 883 (H-13) vs. time at 800°F in argon.

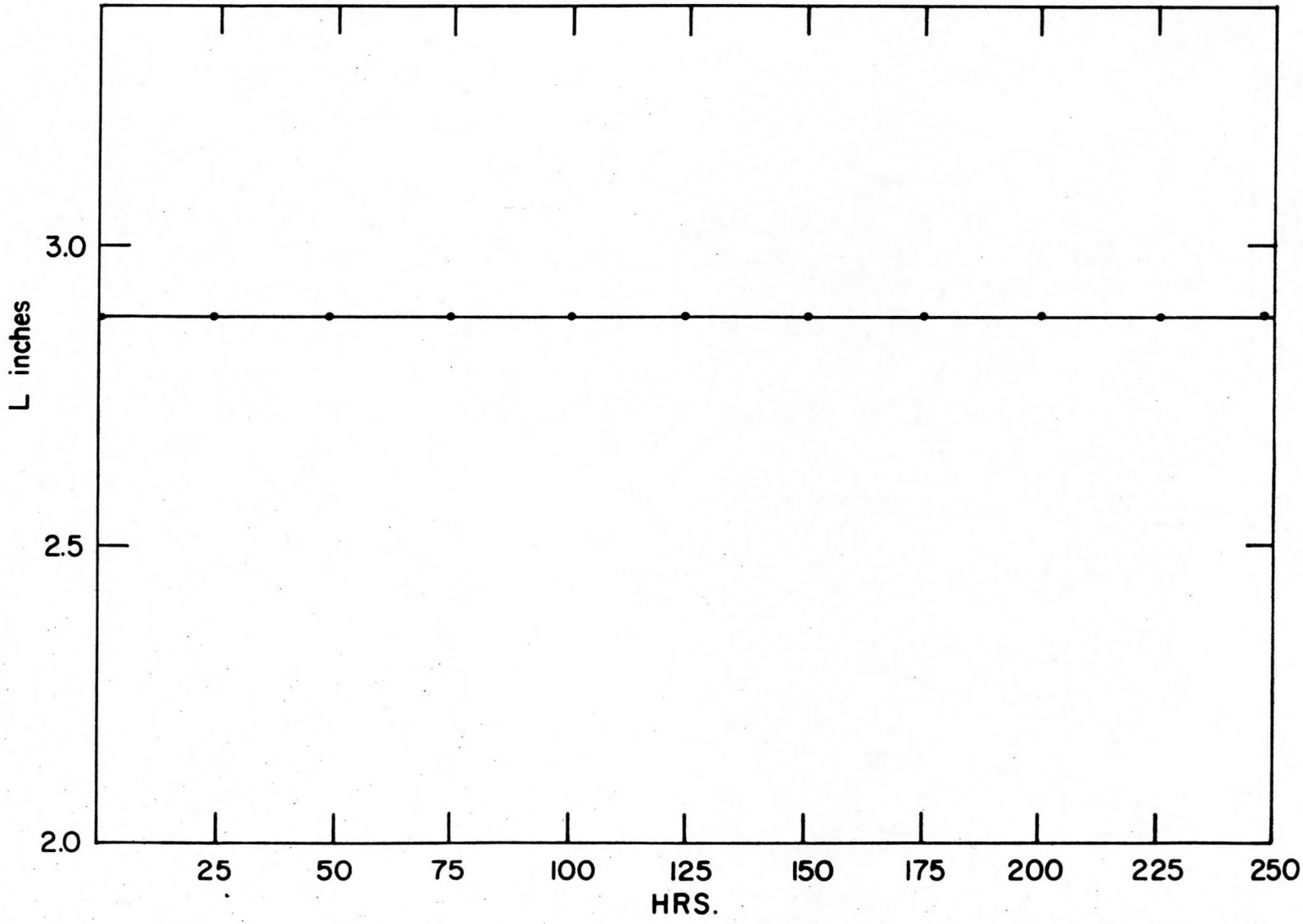

Fig. 3: Plot of thermal stability of A387 vs. time at 1000°F in argon.

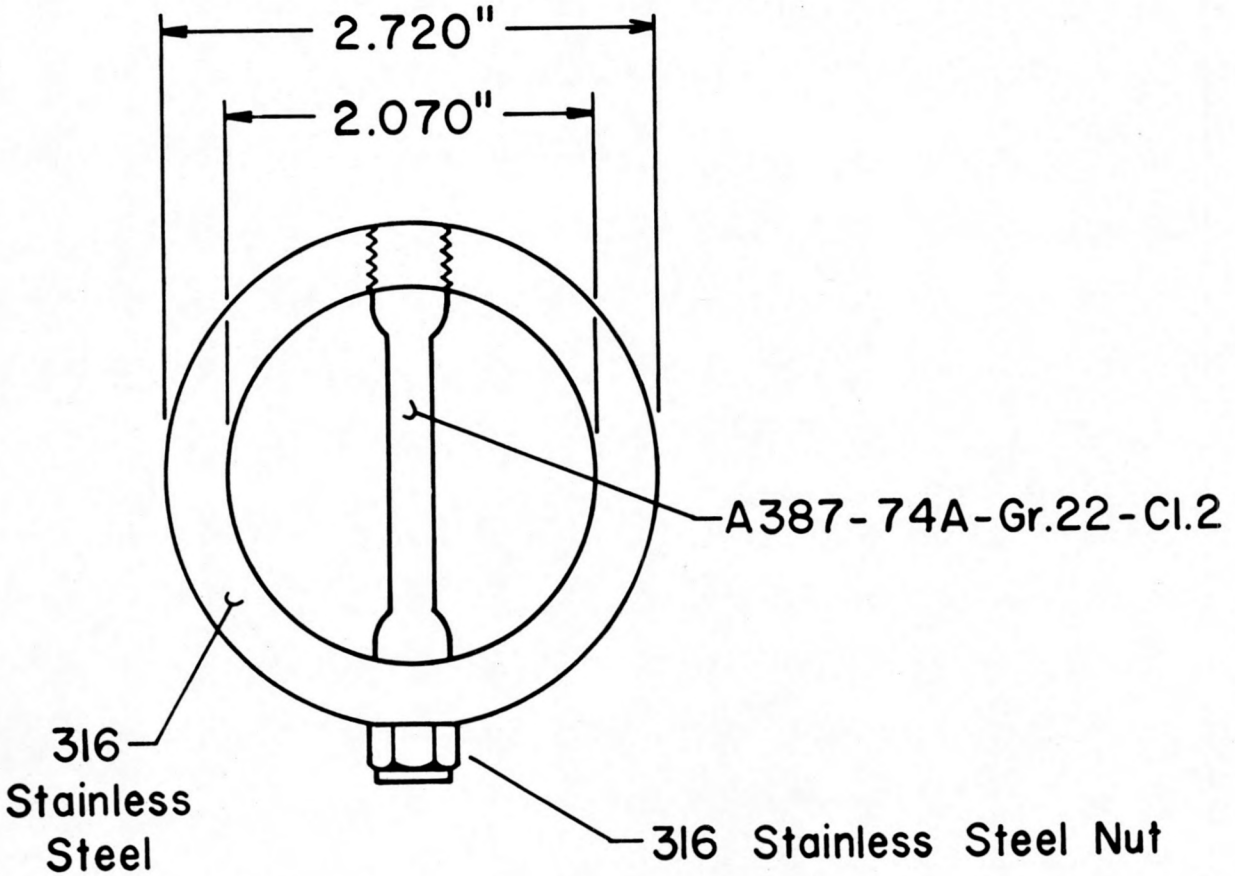

Fig. 4: Ring-Sample Composites for stressed exposures. Rings used in this study have O.D. = 2.554 inches.

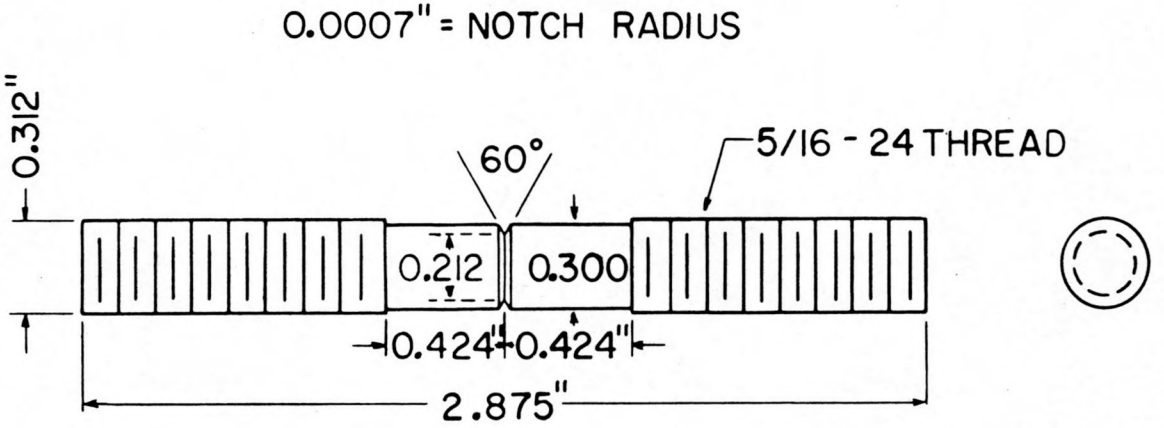

Fig. 5: A387 Notched-Bar Tensile Specimen.

expansion rig and heated to 1000°F in argon gas. The ring-sample composite diameter was monitored as a function of time for 250 hours and is presented in Figure 6. The stress in the sample during the course of the 250 hours is shown in Figure 7. The stress was calculated as shown in the following analysis. The deflection of the ring at 1000°F was given by —

$$\Delta D_{1000} = D_{ring} - D_{comp.} , \qquad (I)$$

where, ΔD_{1000} = ring deflection at 1000°F (or T of interest)

D_{ring} = diameter of the ring alone at 1000°F (or T of interest)

$D_{comp.}$ = measured value of the ring-sample composite diameter at 1000°F (or T of interest).

The diameter of the ring alone at 1000°F was taken to be —

$$D_{ring} = D_o (1 + \alpha_r \Delta T) \qquad (II)$$

where, D_o = ring diameter at room temperature

α_r = ring average thermal expansion coefficient over T range of interest

ΔT = temperature deviation from room T.

Substituting Equation II into Equation I gives —

$$\Delta D_{1000} = D_o (1 + \alpha_r \Delta T) - D_{comp.} \qquad (III)$$

The load exerted by the ring on the specimen was —

$$P = K_r \Delta D_{1000} \qquad (IV)$$

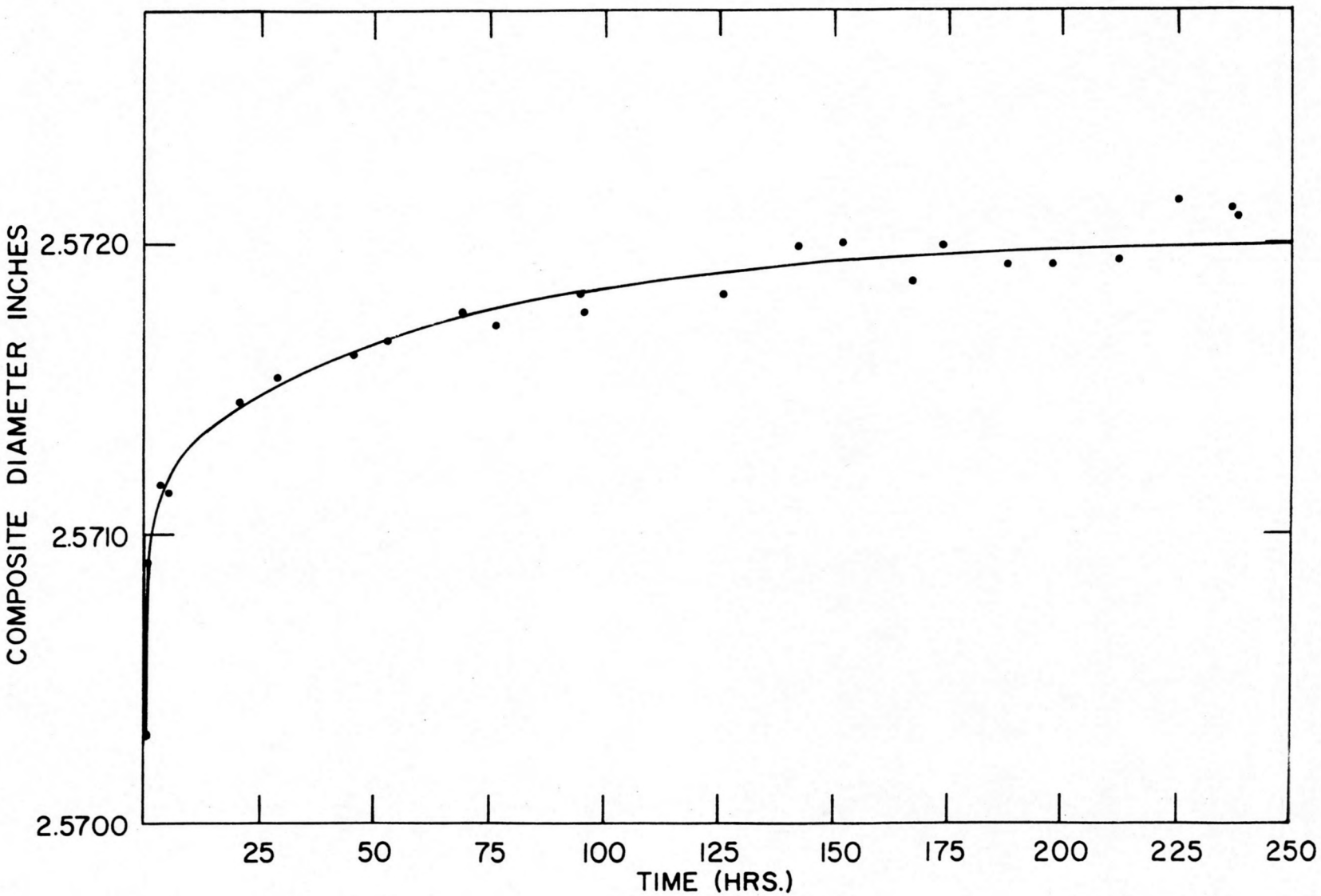

Fig. 6: Ring-Sample Composite relaxation vs. time at 1000°F in argon for an A387 notched-bar specimen initially loaded to 26.4 ksi.

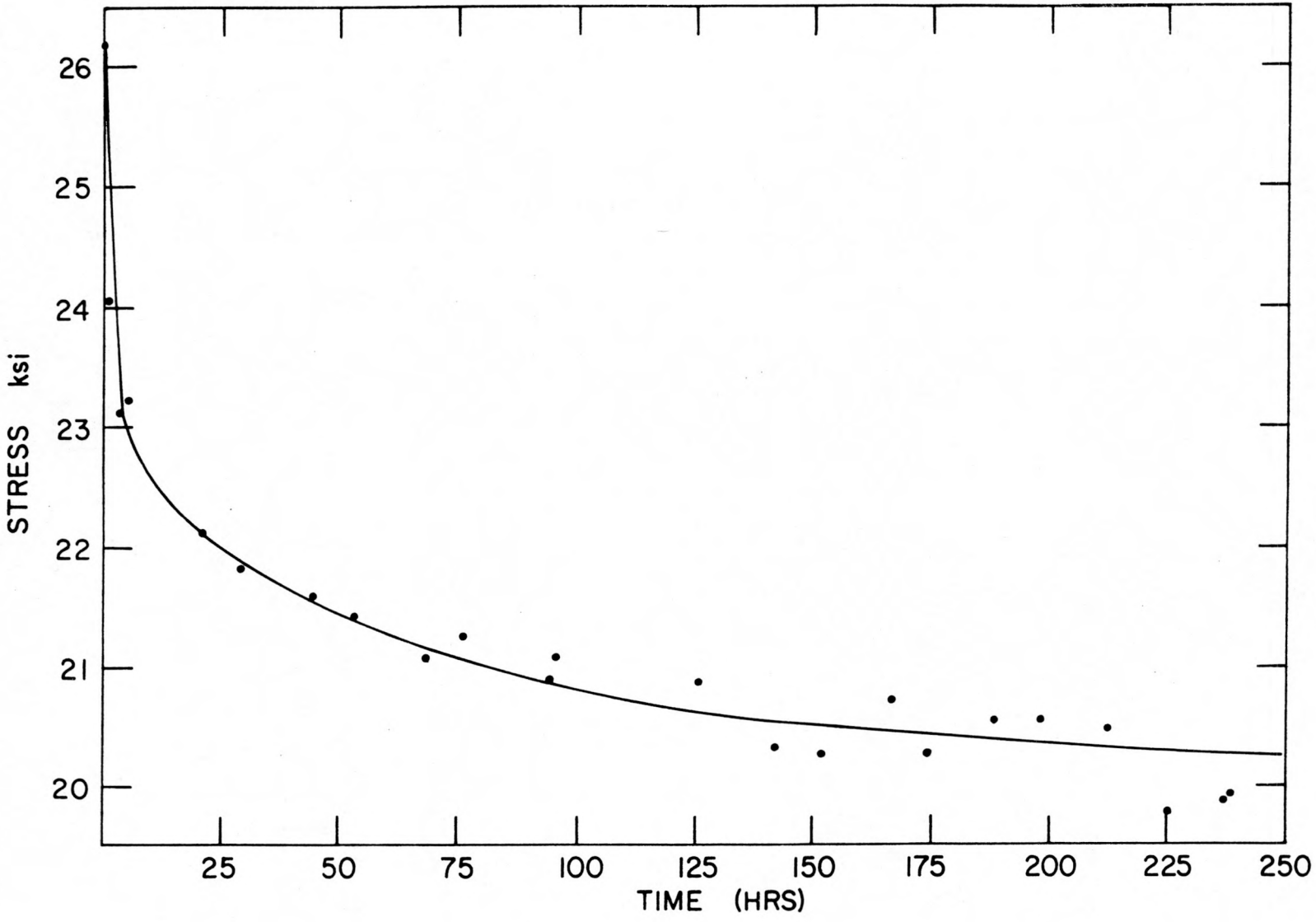

Fig. 7: Sample stress vs. time for an A387 notched-bar tensile specimen, ring loaded at 1000°F in argon.

where, P = Load

K_r = ring compliance coefficient at 1000°F (or T of interest).

The stress was then calculated by dividing the load by the thermally corrected cross-sectional area of the specimen, or —

$$\sigma = P/A \tag{V}$$

where, σ = stress in the specimen

and,

$$A = A_o\ (1 + \alpha_s \Delta T)^2 \tag{VI}$$

where, A = thermally corrected area of specimen

A_o = area at room temperature of specimen

α_s = specimen average thermal expansion coefficient over T range of interest.

Substituting Equations III, IV and VI into V resulted in the equation for the stress in the sample for any measured value of the ring-sample composite diameter —

$$\sigma = \frac{K_r(D_o(1 + \alpha_r \Delta T) - D_{comp.})}{A_o(1 + \alpha_s \Delta T)^2} \ . \tag{VII}$$

If the problem is treated as one of elastic equilibrium between two bodies (i.e. the sample and the ring) undergoing a thermal deviation from room temperature, the following equation of equilibrium is obtained —

$$\Delta D_T = \frac{\frac{A\ E}{\ell_\varepsilon}\ (D_o - \ell_s + \alpha_r D_o \Delta T - \alpha_s \ell_s \Delta T)}{K_r + \frac{A\ E}{\ell_\varepsilon}} \tag{VIII}$$

where, ΔD_T = theoretical ring deflection at T of interest

E = Young's modulus of specimen at T of interest

ℓ_ε = straining gage length of specimen (effective gage length), thermally corrected

ℓ_s = length of specimen loaded in ring, this is a function of the initial room temperature ring deflection.

The derivation of Equation VIII is too lengthy to be presented here. However, the theoretically calculated value of deflection for a ring-sample composite having an initial room temperature deflection of 1.7×10^{-3} inches and heated to 1000°F is 7.63×10^{-3} inches. The experimentally determined value of ring deflection for the same conditions was 7.56×10^{-3} inches. Since the standard error is found to be $\pm 0.1 \times 10^{-3}$ inches for both cases, the difference is meaningless. The agreement between theory and experiment is very good.

Calibration curves of compression load versus deflection were determined for diametrically loaded rings of 316 stainless steel (Fig. 8). Tests were carried out in argon at 76, 200, 400, 600, 820 and 1000°F. Results are shown in Figure 9. Ring compliance coefficients were determined from the slopes of the load-deflection curves. The results are plotted versus temperature in Figure 10. The compliance coefficients showed linear behavior with temperature.

Compact tension specimens (CTS) (Fig. 11) and bolt loaded compact tension specimens (Fig. 1) were prepared from a 0.75 inch thick hot rolled plate of A387-74A-Gr.22-Cl.2 steel. The starter notch was machined perpendicular to the rolling direction (ASTM specification E-399, L-T type specimen). The surface of the specimens was mechanically polished to 600 grit.

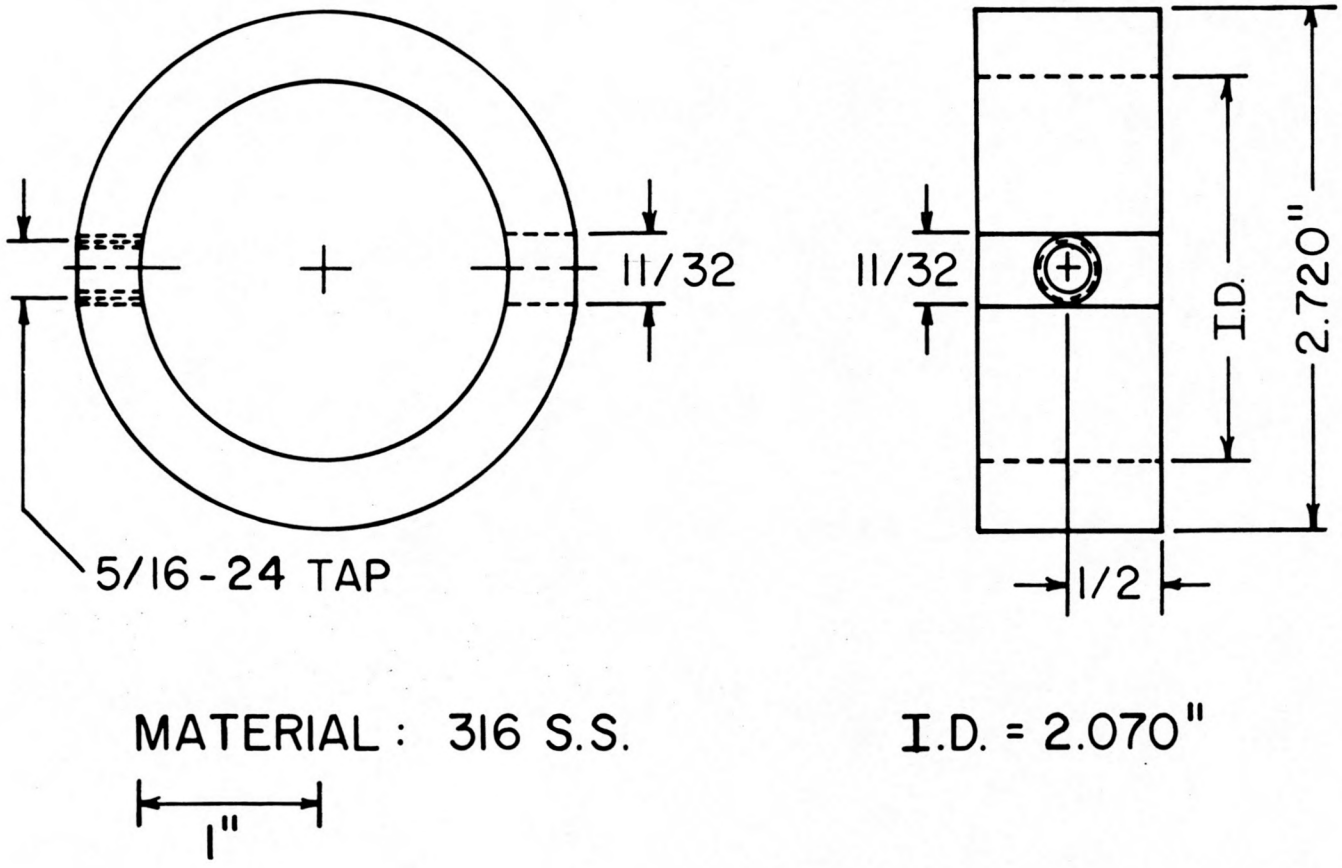

Fig. 8: 316 SS Loading Ring. Rings used in this study have O.D. = 2.554 inches.

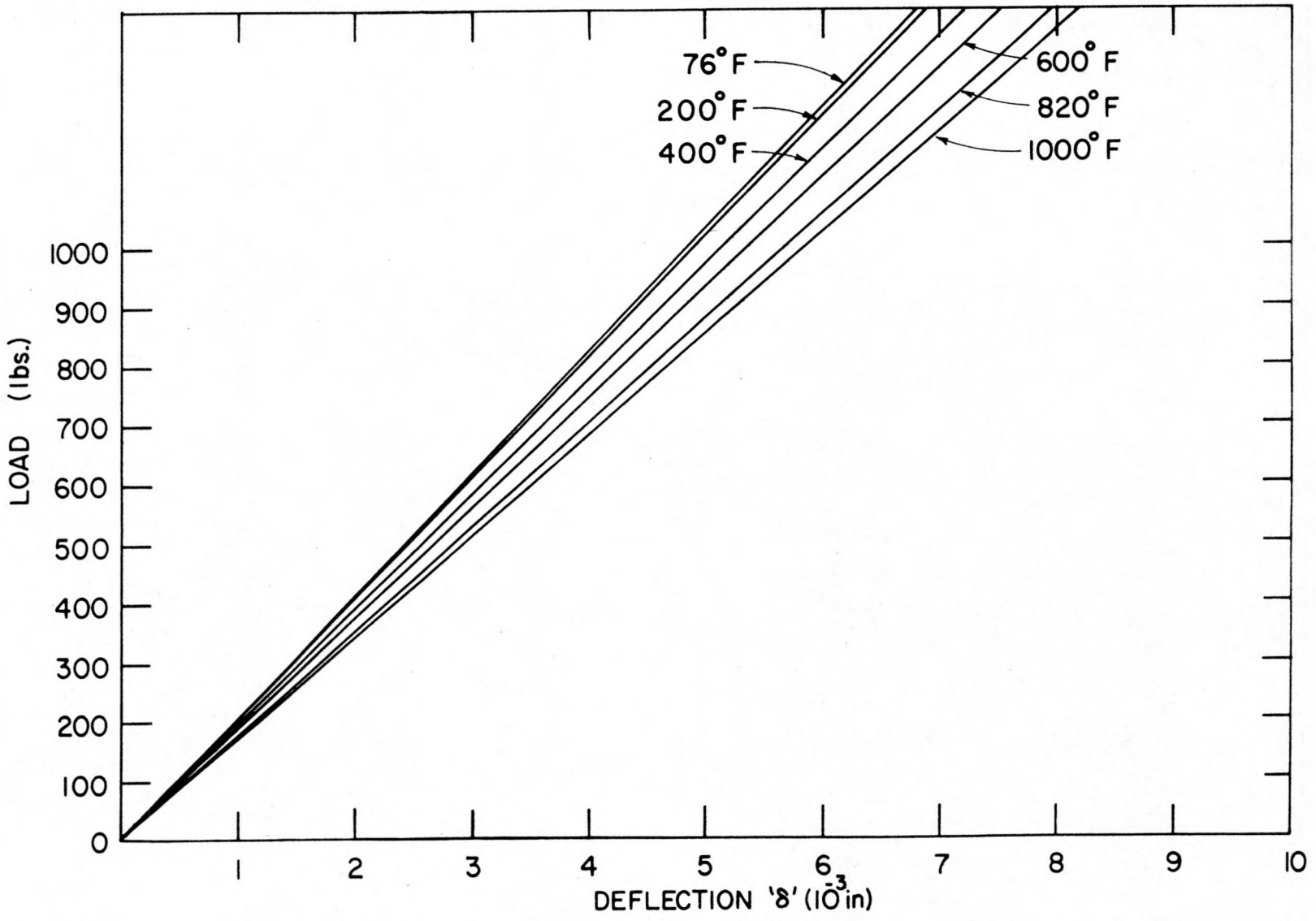

Fig. 9: 316 SS ring deflection vs. compression load calibration curves.

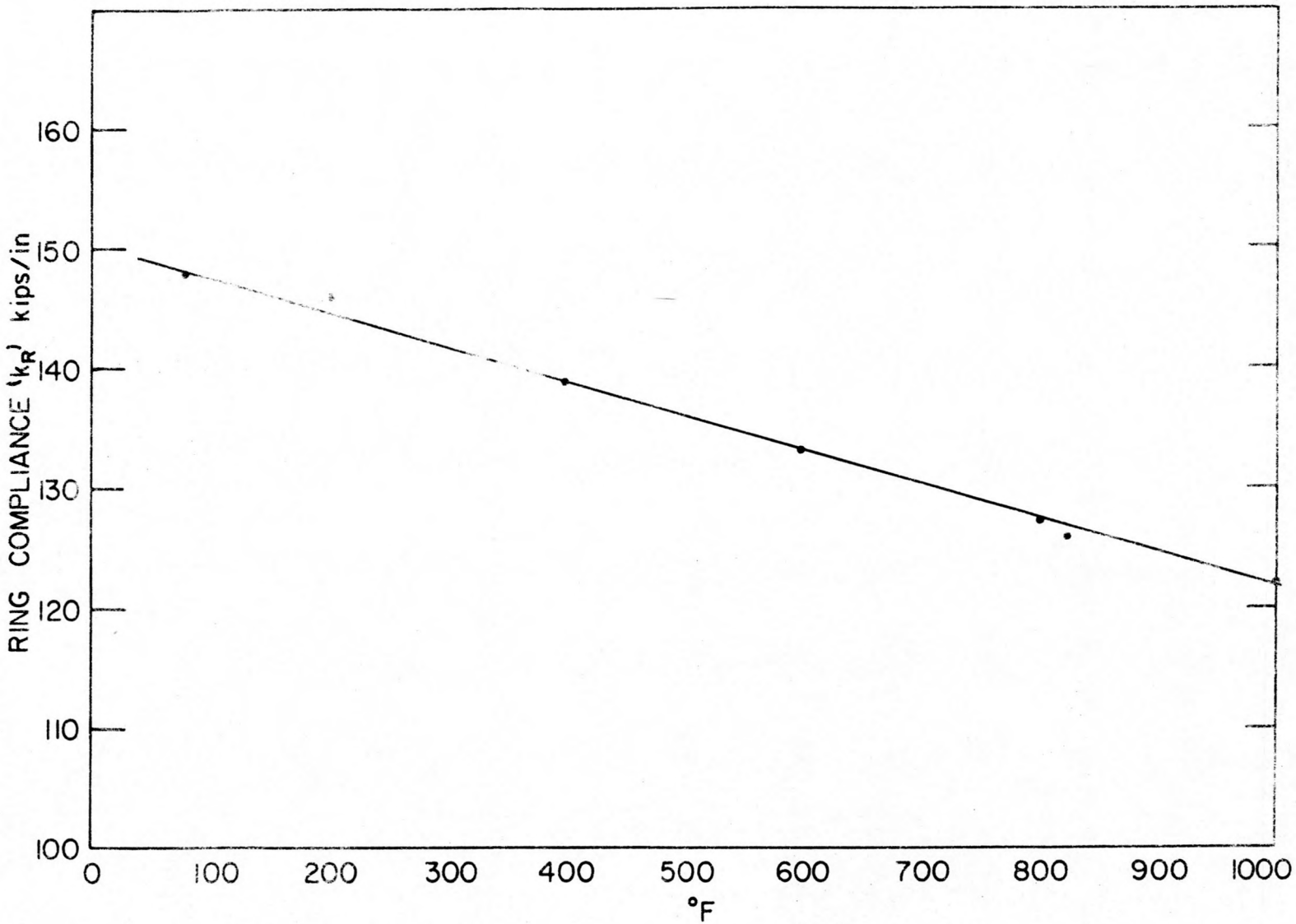

Fig. 10: 316 SS ring compliance coefficients vs. temperature.

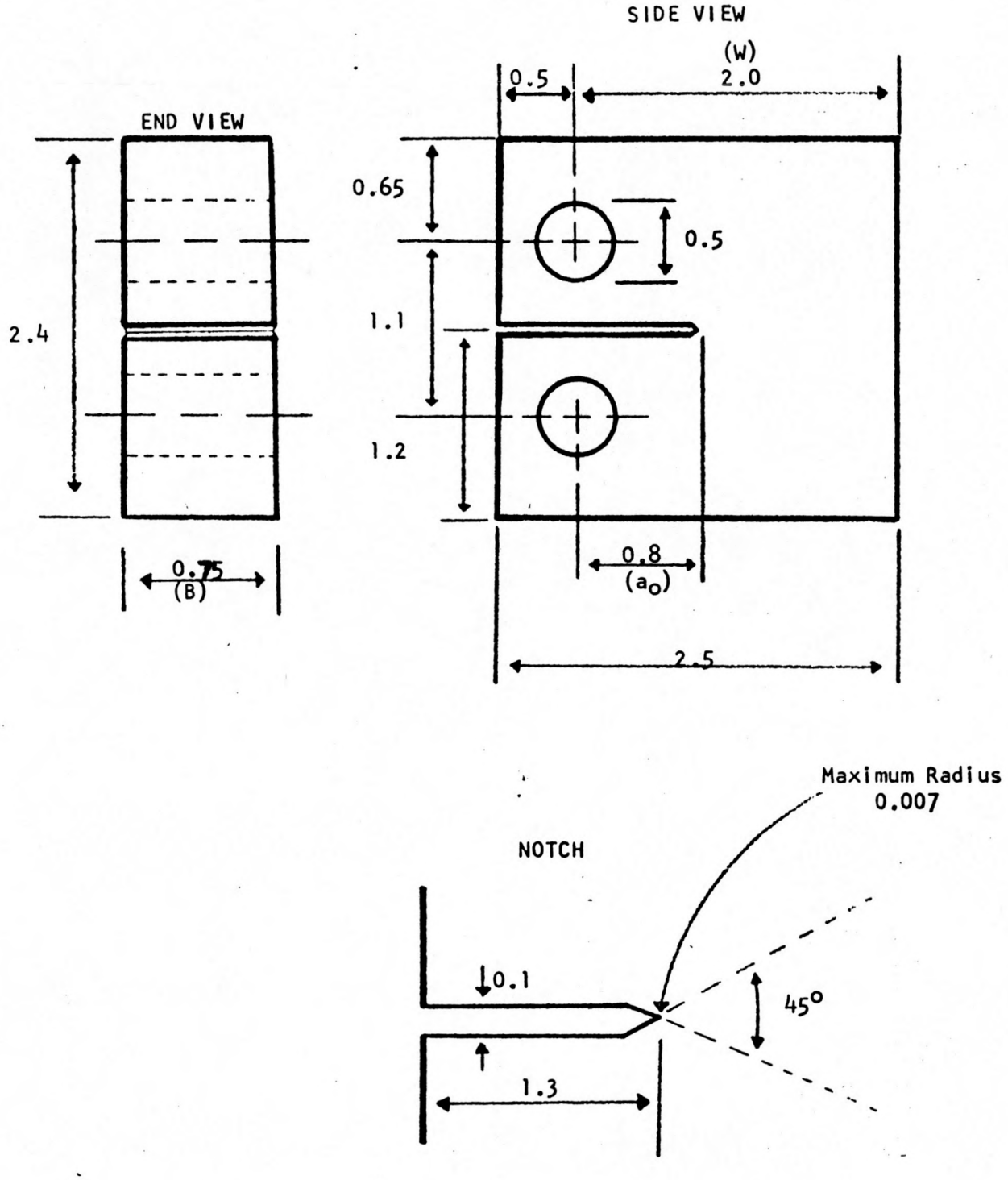

Fig. 11: 2 1/4 Cr-1 Mo Compact Tension Specimen. All dimensions are in inches.

Three bolt loaded specimens were precracked to a total crack length, 'a' (as measured from the load line to the tip of the precrack), of 1.1843, 1.1950 and 1.2412 inches respectively using an MTS-series 810 electro-hydraulic test system. The precracking was done in load control. The frequency was 20 Hz. and the loading was sinusoidal in a tension-tension mode with the minimum load controlled at 10% of the maximum load. The maximum load criterion was derived as shown in the following analysis. The ASTM E-399 fatigue precracking procedure requires that —

$$K_{f\ max} \leq 0.002\ E\sqrt{in} \quad .$$

However for the CTS, K_f is given by —

$$K_f = (P/B\sqrt{a})\ f(\frac{a}{w}) \ .$$

Rewriting the preceding equation in terms of maximum load gives —

$$P_{max} = \frac{K_{f\ max}(B\sqrt{a})}{f(a/w)} \quad .$$

Inserting the ASTM E-399 condition for $K_{f\ max}$ as given above leads to the maximum load criterion —

$$P_{max} \leq 0.002\ E\ (\frac{B\sqrt{a}}{f(a/w)}) \quad ,$$

where, $K_{f\ max}$ = maximum stress intensity of the fatigue cycle

E = Young's modulus

P = load

B = specimen thickness

a = crack length

f(a/w) = measure of the compliance of the specimen.

P_{max}, for each of the three specimens, was chosen as the greatest value of load that satisfies the inequality at 'a' equal to 1.1843, 1.1950 and 1.2412 inches respectively.

Compliance curves were determined at room temperature for all three BLCTS and at 800°F for the two specimens with the longest total crack length. The compliance was measured at the notch front face (A, Fig. 1). Results are presented in Figure 12. The ratio of the slopes of the compliance curves at 800°F to those at room temperature for each respective crack length equals (within experimental error) the ratio of Young's modulus of the material for the two temperatures.

II. Fracture Mechanics Tests

A. Procedure and Results:

Fatigue crack growth rates (da/dN) were determined as a function of stress intensity range (ΔK) in moist ($\sim$30%RH) air at ambient temperature and pressure. ΔK was calculated as follows:

$$\Delta K = (P_{max} - P_{min}) \frac{f(a/w)}{B\sqrt{a}}$$

where, P_{max} = maximum load of fatigue cycle

P_{min} = minimum load of fatigue cycle.

A compact tension specimen was precracked to a total crack length of 0.85 inches using the procedure outlined in Section I. The precracked specimen was then cycled at 20 Hz. in load control at a ΔK value of 10 ksi $\sqrt{in}$. The loading was sinusoidal with P_{min} controlled at 10% of P_{max} ($R=0.1=P_{min}/P_{max}$). The loading was carried out until the crack growth rate was detected to be uniform over moderate periods of time. This assured that the

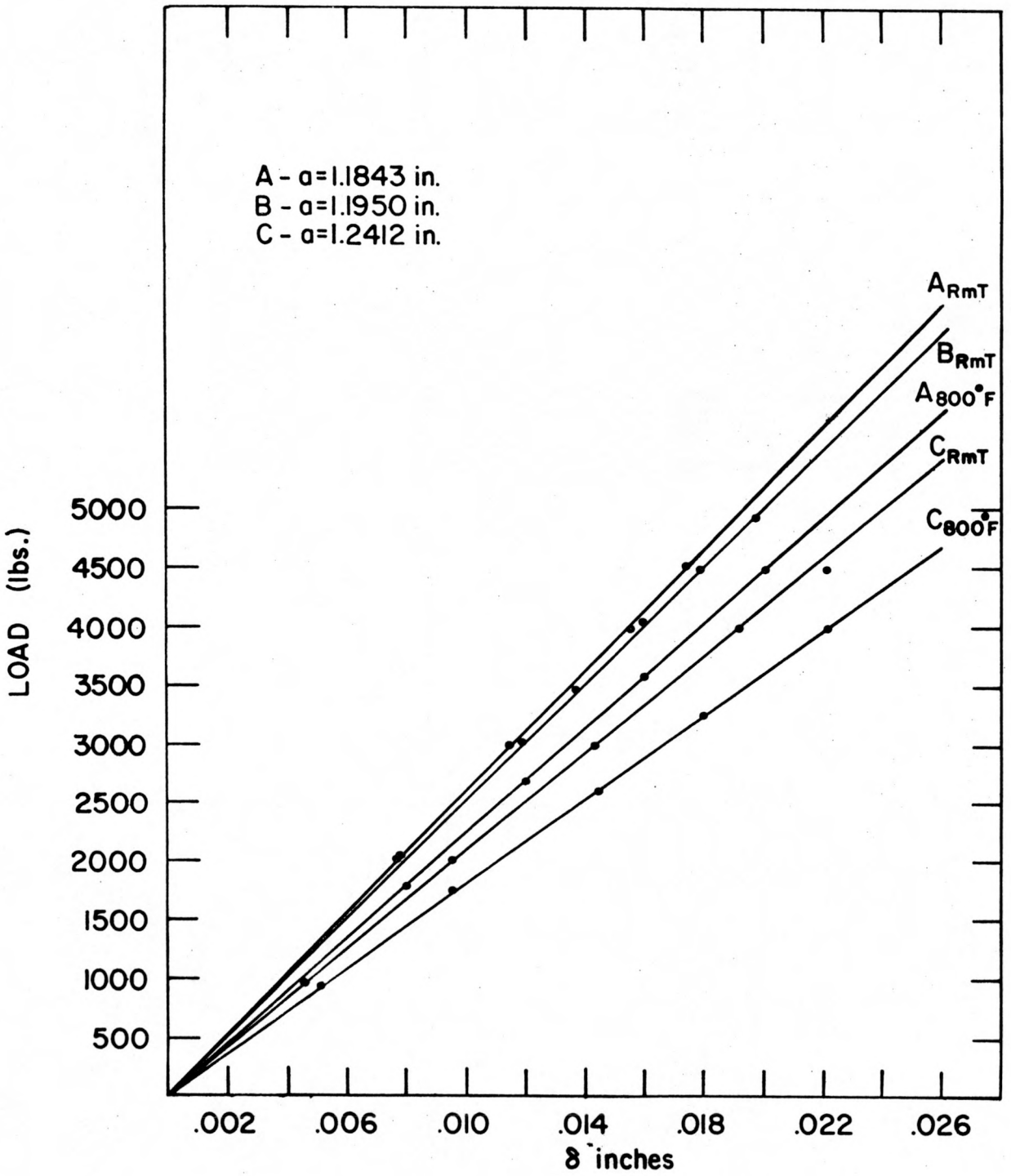

Fig. 12: Load vs. compliance (measured at the notch front face) for bolt-loaded compact tension specimens of different crack lengths (a).

plasticity ahead of the crack due to the precracking procedure would not affect the determination of the stress intensity threshold (ΔK_{TH}). The stress intensity range was decreased in 10% increments until crack growth could not be detected in 2×10^5 cycles. Since the resolution of the crack growth measurement system is $\sim \pm 1$ mil, this corresponds to a crack growth rate of 5×10^{-9} in./cycle. This was termed the stress intensity threshold. ΔK_{TH} was determined to be 8.5 ksi $\sqrt{in}$ in moist air at ambient temperature and pressure. Fatigue crack growth rates were then determined for ΔK values ranging from threshold to $\sim$40 ksi $\sqrt{in}$. The results were plotted as log da/dN vs log ΔK (Fig. 13).

The same test, as outlined above, was repeated in hydrogen gas at 15 psig and ambient temperature. ΔK_{TH} was lowered to 6.5 ksi $\sqrt{in}$ due to the presence of the hydrogen gas. Crack growth rates (da/dN) above ΔK values of $\sim$10 ksi $\sqrt{in}$ were not appreciably affected by the presence of hydrogen gas (Fig. 13).

Two bolt loaded compact tension specimens (Fig. 1) were loaded at room temperature to a predetermined value of K (stress intensity). The specimens were placed in a 304 stainless steel can containing coal slurry. One sample was immersed in the slurry and the other was suspended above the slurry. The coal slurry was a blend of 35 volume percent of -100 mesh Kentucky bituminous (Proximate Analysis, wt.pct.: Moisture, 6.1; Ash, 15.5; Volatile Matter, 36.3; Fixed Carbon, 42.1) and 65 volume percent solvent. The sulfur content of the coal was 5.53 wt.pct. The solvent was centrifuged Synthoil product (Ash free wt.pct.: Organic benzene insols, 3.3; asphaltenes, 32.3; Oils, 64.4) from PERC Run FB-61 made from the coal described above. The coal and solvent were graciously supplied by Paul M. Yavorsky of PERC. The

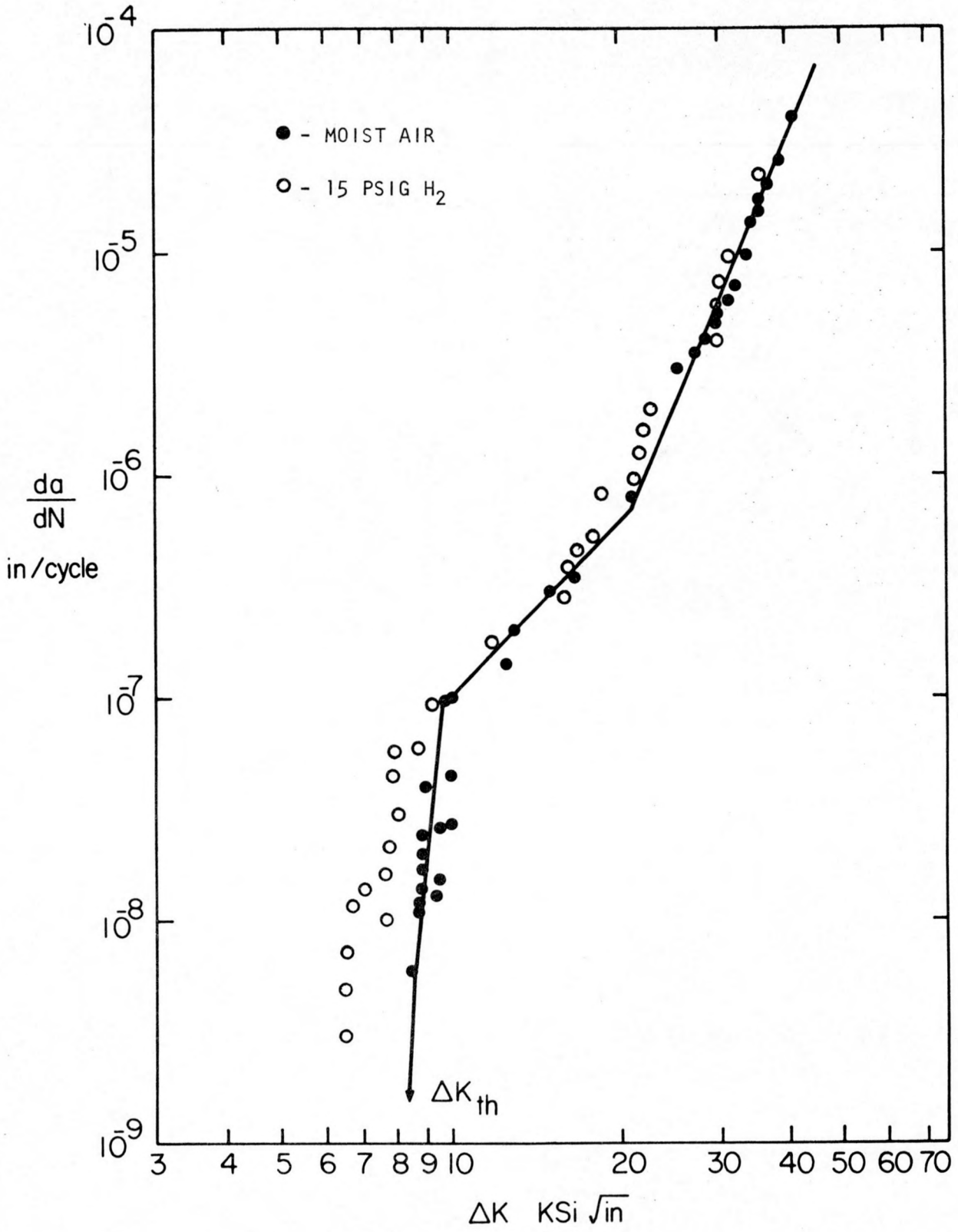

Fig. 13: Fatigue crack growth rate curves for 2 1/4 Cr-1 Mo steel in moist air (~30% R.H.) or 15 psig H_2 at ambient temperature.

slurry was prepared by mixing the fine coal in the solvent which, because of its high viscosity (161 SSF at 180°F) at room temperature, was preheated to 110°F. The can was placed in a pressure vessel, 1500 psig H_2 was pumped in and the system was equilibrated to 800°F, 4000 psig total pressure.

The K value at temperature was calculated in very much the same manner as the stress was calculated for the ring-sample composites. The problem was treated as two elastic bodies in static equilibrium undergoing a temperature deviation from room temperature. The equilibrium notch-front-face (NFF) displacement (at 800°F) was calculated to be —

$$\Delta\ell_{NT} = \frac{(\ell_B - \ell_N + \alpha_B \ell_B \Delta T - \alpha_N \ell_N \Delta T) E_B A_B}{K_{NT}(\ell_B + \alpha_B \ell_B \Delta T) + E_B A_B}$$

where,

$\Delta\ell_{NT}$ = notch-front-face displacement at T

ℓ_B = straining portion of the loading bolt, this is a function of the room temperature NFF displacement

ℓ_N = notch gap length at room temperature

α_B = bolt material average thermal expansion coefficient for T range of interest

α_N = BLCTS material average thermal expansion coefficient for T range of interest

ΔT = temperature deviation (T - RmT)

E_B = Young's modulus of bolt material at T

A_B = bolt area at T

K_{NT} = BLCTS compliance coefficient at T (for initial crack length 'a'.).

The derivation of this equation is too lengthy to be presented here. The load exerted on the BLCTS by the bolt was calculated from —

$$P = K_{NT} \Delta\ell_{NT} .$$

The stress intensity (K) was obtained from —

$$K = (P/B\sqrt{a})\ f(\frac{a}{w}) .$$

The two specimens were loaded to K values of 62.2 and 71.7 ksi$\sqrt{in}$ respectively at temperature (800°F) at the beginning of the test. The test was scheduled to last 350 hours. Unfortunately a rupture disk failure caused termination of the test at ∿200 hours. No crack extension was observed. Further analysis of the specimens has not yet been performed.

III. Hydrogen Attack Tests

A. Procedure:

Smooth-bar (Fig. 14) and notched-bar (Fig. 5) tensile specimens of A387-74A-Gr.22-Cl.2 steel were prepared from longitudinal (parallel to the rolling direction) sections of the plate. Six smooth-bar and six notched-bar specimens were exposed to 4000 psig hydrogen gas at 1000°F for 500 hours. Three of each type of specimen were loaded under stress via precompressed stainless steel loading rings. Nine notched-bar specimens were exposed to 4000 psig hydrogen gas at 1000°F for 250 hours. Three specimens were stressed and six were unstressed during exposure. Three of the six unstressed samples had been prestrained (ε_p = 0.92%) in air at room temperature prior to the exposure. Three smooth-bar specimens were exposed unstressed to 4000 psig hydrogen gas at 1000°F for 168 hours.

Each type of exposure mentioned above was done in three specimen lots. After the exposure the specimens were removed from the pressure vessel for

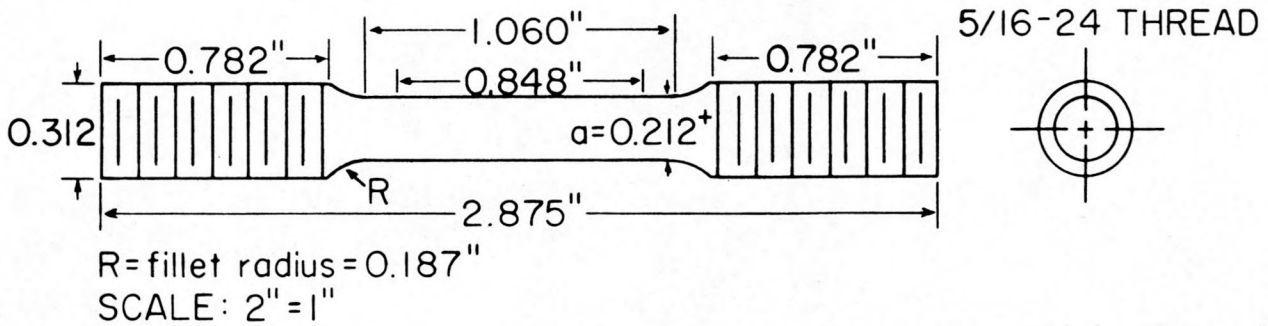

Fig. 14: A387 Smooth-Bar Tensile Specimen.

analysis. One specimen of each lot was mounted in copper conducting bakelite and polished to Linde B (0.05 μ particle size) for micrographic analyses. The other two specimens of the lot were tensile tested at room temperature in air on a TT-C Instron tensile test machine.

Sample lengths, diameters and ring-sample diameters were measured before and after the exposure. The stress in the stressed samples was calculated by —

$$\sigma = \frac{K_r \Delta D_T}{A} \qquad \text{(see Section I)},$$

ΔD_T was determined from measurements of ring deflection at the start and end of each exposure and by use of Equation VIII.

Metallographic analyses were performed both optically and with a scanning electron microscope (SEM). Surfaces were examined as polished and after etching for ∿10 seconds with a 2% Nital solution (2% HNO_3 in methanol).

B. Results:

Results of the mechanical properties tests on A387-74A-Gr.22-Cl.2 steel smooth-bar tensile samples pre-exposed to 4000 psig hydrogen gas at 1000°F are presented in Table 2. None of the room temperature mechanical properties were affected even after 500 hours of exposure.

Results of the mechanical properties tests on notched-bar samples of the same steel exposed to the same conditions of temperature and H_2 pressure as given above are presented in Table 3. No significant loss of notch tensile strength was observed except for the 500 hour stressed exposures. Considerable differences were noted in reduction of area (R.A.) for specimens exposed under conditions of stress and pre-strain. The 250 hour

TABLE #2

MECHANICAL PROPERTIES TESTS

2 1/4 Cr-1 Mo steel smooth-bar tensile samples pre-exposed to 4000 psig H_2 at 1000°F

Test conditions: T=72°F P=1 atm air $\dot{\varepsilon}=0.05\ min^{-1}$

Type of Exposure	Exposure Time (Hrs.)	Stress* (ksi)	ΔL/Lo** (%)	ΔD/Do*** (%)	0.2%Y.S. (ksi)	U.T.S. (ksi)	T.E. (%)	R.A. (%)
None (as-received)	---	----	----	--	78.7	95.6	24.7	75.5
Unstressed	168	----	0	0	79.5	96.0	23.2	74.2
Unstressed	500	----	0	0	78.5	95.0	23.0	75.4
Stressed	500	30.2 to 17.8	0.35	∿0	76.5	93.0	23.7	74.2

* Applied by pre-compressed loading rings. Values are for start of run and end of run.

** Change in sample length during exposure divided by sample gage length (1").

*** Change in sample gage diameter during exposure divided by original gage diameter.

TABLE #3

MECHANICAL PROPERTIES TESTS

2 1/4 Cr-1 Mo steel notched-bar tensile samples pre-exposed to 4000 psig H_2 at 1000°F

Test conditions: T=72°F P=1 atm air $\dot{\varepsilon}=0.05\ min^{-1}$

Type of Exposure	Gas	Exposure Time (Hrs.)	Stress* (ksi)	ΔL/Lo** (%)	ΔD/Do*** (%)	N.T.S. (ksi)	R.A. (%)
None (as-received)	-----	---	----	----	----	148.2	25.0
Unstressed	H_2	250	----	0	+0.14	148.6	25.3
Stressed	H_2	250	26.4 to 19.4	+0.07	+0.05	147.3	20.4
Prestrained (0.92%)	H_2	250	----	0	+0.05	145.4	17.7
Unstressed	H_2	500	----	0	----	148.0	21.0
Stressed	H_2	500	31.2 to 19.7	+0.12	----	128.0	11.0
Unstressed	Argon	250	----	0	0	148.2	26.1
Stressed	Argon	250	26.4 to 20.1	+0.06	0	149.4	25.3
Prestrained (0.92%)	Argon	14	----	0	0	149.8	23.7

* Applied by pre-compressed loading rings. Values are for start of run and end of run.

** Change in sample length during exposure divided by total sample length (∿2.86").

*** Change in sample notch-diameter during exposure divided by original notch-diameter.

exposures showed no difference between R.A.'s for unstressed specimens exposed to argon or hydrogen. The stressed specimens exhibited ∿20% less R.A. for specimens exposed to hydrogen than those exposed to argon. The prestrained samples showed ∿25% less R.A. for samples exposed to hydrogen than those exposed to argon. The 500 hour exposures exhibited degradation for both the unstressed and stressed samples. There was no loss of strength for the unstressed samples. The stressed samples showed ∿13.5% less notch tensile strength than the as-received material. The reduction in area of the unstressed samples decreased by ∿16%, while the stressed samples showed ∿56% less reduction in area.

Metallographic analyses of all the 250 hour and 500 hour exposures to hydrogen, at the given conditions, revealed the formation of small methane bubbles in or near grain boundaries and second phase precipitates. The highest concentration of bubbles was observed in the vicinity of the notch of stressed samples where the triaxiality of stress was greatest. Figures 15, 16 and 17 illustrate the above very well.

In summary, smooth-bar tensile specimens showed no significant changes in any of the room temperature mechanical properties even though methane bubbles were detected in or around grain boundaries and second phase particles. Notched-bar specimens, however, showed marked changes in many of the room temperature mechanical properties. Methane bubbles formed more readily in regions of high stress triaxiality. The great loss of reduction in area for the prestrained samples indicates that it may be strain and not stress that causes the increased amount of hydrogen attack in the vicinity of the notch.

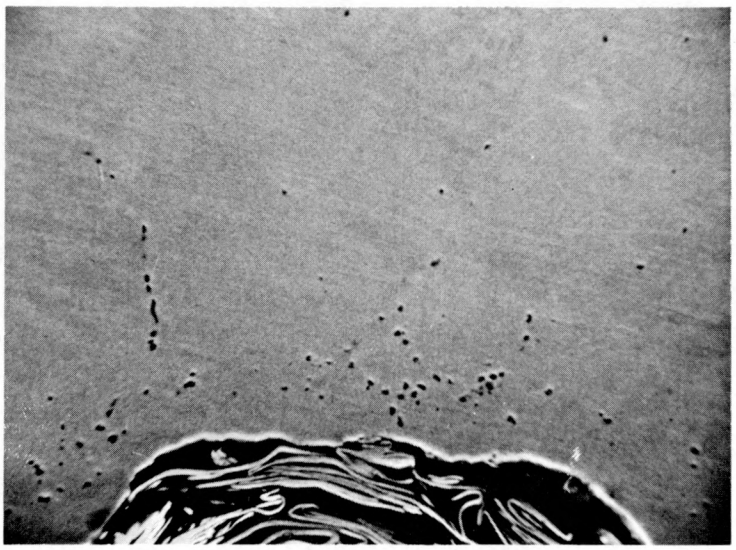

Fig. 15: Scanning electron micrograph showing high density of bubbles in region of notch for A387 notched-bar tensile specimen exposed with stress for 500 hours to 4000 psig H_2 gas at 1000°F. (1260X)

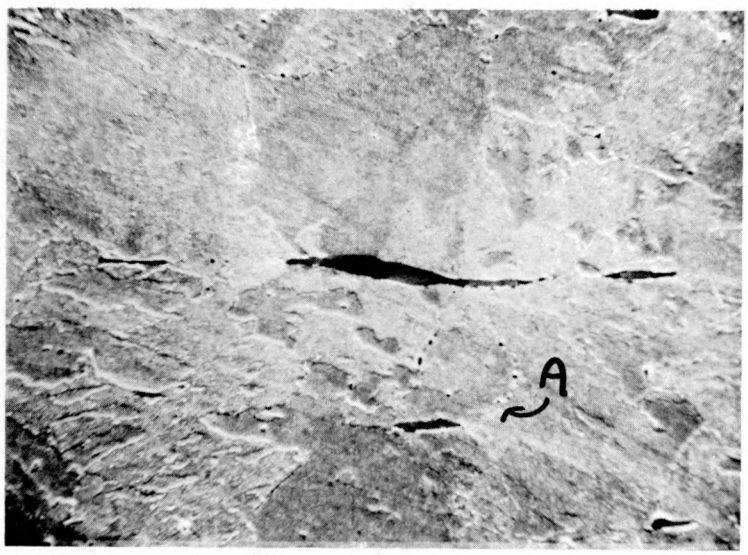

Fig. 16: Scanning electron micrograph of bulk region away from notch for specimen of Figure 15. Surface was etched with 2% Nital (~10 sec.). Bubbles are visible in grain boundaries and near the manganese sulfide precipitates. (1000X)

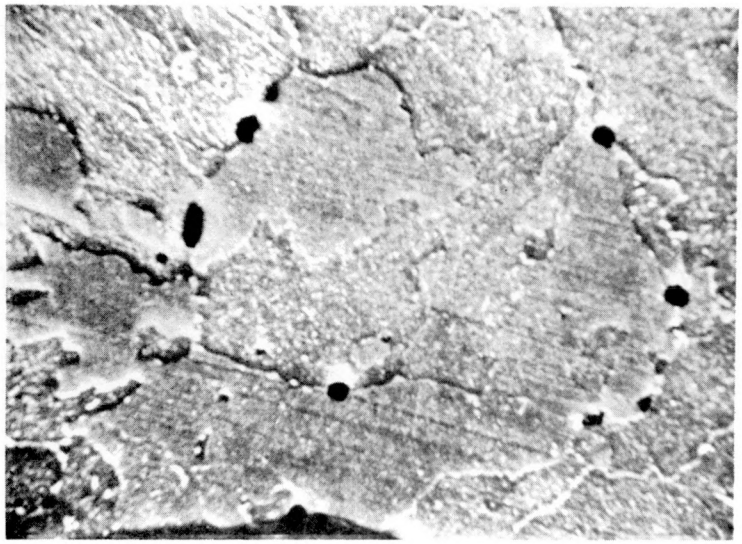

Fig. 17: Scanning electron micrograph of region A in Figure 16 at higher magnification (5000X). Shows bubbles in grain boundaries and on interface between manganese sulfide inclusion and bulk matrix (bottom center).

Distribution List for Technical Reports

Name and Address

S. J. Dapkunas (2)
Department of Energy
Div. of Planning and Systems Engineering
Mail Stop C-156 (GTN)
Washington, D.C. 20545

R. A. Bradley, Manager (4)
Fossil Energy Materials Project
Oak Ridge National Laboratory
P. O. Box X
Oak Ridge, TN 37830

S. J. Schneider (2)
National Bureau of Standards
Department of Commerce
Washington, D.C. 20234

E. E. Hoffman, Chief (1)
Energy Materials and Systems Branch
Oak Ridge Operations Office
Department of Energy
P. O. Box E
Oak Ridge, TN 37830

Richard Schorr (1)
Battelle Columbus Lab
505 King Avenue
Columbus, OH 43201

R. P. Wei (1)
Lehigh University
Center for Surface and Coatings Branch
Bethlehem, PA 18015

Dilip Bhandarkar (1)
Lawrence Berkeley Laboratory
University of California
Berkeley, CA 94720

D. Canonico (1)
Oak Ridge National Laboratory
P. O. Box X
Oak Ridge, TN 37830

Technical Information Center (245)
Department of Energy
Oak Ridge, TN 37830

J. Slaughter (1)
Oak Ridge National Laboratory
P. O. Box X
Oak Ridge, TN 37830

W. J. Lochmann (1)
The Ralph M. Parsons Co.
100 West Walnut Street
Pasadena, CA 91124

G. Sorell (1)
Exxon Research and Engineering Company
P. O. Box 101
Florham Park, NJ 07932

William E. Erwin (1)
Engineering Department
Standard Oil Company of California
P. O. Box 1272
Richmond, CA 94802

G. Catus (1)
109 Office & Laboratory
Ames Laboratory
Iowa State University
Ames, IA 50011

R. Fisher (2)
321 Spedding
Ames Laboratory
Iowa State University
Ames, IA 50011

T. Scott (5)
126 Metals Development Building
Ames Laboratory
Iowa State University
Ames, IA 50011

Charles M. Woods (10)
204 Metals Development Building
Ames Laboratory
Iowa State University
Ames, IA 50011

Burton Gleason (10)
201 Spedding
Ames Laboratory
Iowa State University
Ames, IA 50011